OCTANT ANALYSIS BASED STRUCTURAL RELATIONS FOR THREE-DIMENSIONAL TURBULENT BOUNDARY LAYERS

Semih M. Ölçmen[1] , Roger L. Simpson[2] and Jonathan W. Newby[1]

[1]Aerospace Engineering and Mechanics Department
The University of Alabama
Tuscaloosa, Alabama 35487, USA
newby004@bama.ua.edu, solcmen@coe.eng.ua.edu

[2]Aerospace and Ocean Engineering Department
Virginia Tech
Blacksburg, Virginia 24061, USA
simpson@aoe.vt.edu

ABSTRACT

A flow structure based triple-product correlation model developed by Nagano and Tagawa (1990) has been expanded to three-dimensional turbulent flows. Three-dimensional turbulent boundary layer data obtained away from the vortex in a wing-body junction flow are analyzed to calculate the contributions from eight velocity octants to the stresses and higher order products. The analysis showed that the sweep and ejection modes dominate the flow physics of the shear stresses and some triple products, while the interaction modes are negligible away from the wall. These results are used to extend Naganao and Tagawa's model to obtain correlations between triple products in three-dimensional turbulent boundary layers (3DTBL).

INTRODUCTION

Reynolds averaged Navier-Stokes equations require modeling of the triple products among other terms. Many turbulence diffusion models used in CFD codes, such as the models Daly-Harlow (1970), Hanjalic-Launder (1972), Mellor-Herring (1973), and Lumley (1978), can be found in the literature. These models use the shear stresses, the gradient of the shear stresses, turbulent kinetic energy dissipation rate and the turbulent kinetic energy values to express the triple products. Experimental testing of these models such as given by Schwarz and Bradshaw (1994) for a three-dimensional turbulent boundary layer (3DTBL) by Lemay et al. (1995) in a manipulated 2DTBL show that some of these models (Daly-Harlow and Mellor-Herring) are in good agreement only above $y^+ \approx 150$. These models require the turbulent-kinetic energy dissipation rate term as input, which results in large errors between the prediction and the data (Olcmen and Simpson, 1997).

The main motivation behind the current work was to gain more insights to the structure of the triple products and to obtain equations among the triple products that can simplify the turbulent diffusion modeling used in Reynolds-Averaged Navier-Stokes equations. An analysis based on the work by Nagano and Tagawa (1988, 1990) has been applied to data obtained at seven stations in a wing-body junction flow (Figure 1) to investigate extending their analysis to three-dimensional (3D) flows.

DESCRIPTION OF THE FLOW

The data used here were obtained at Virginia Tech in 1995. The wing shape used in the study had a 3:2 elliptical nose and NACA 0020 tail joined at the maximum thickness t = 7.17 cm. The approach nominal reference velocity of air flow was 27.5 m/sec (Re_θ=5940) (Figure 1).

In a wing-body junction flow the approach wall boundary layer separates from the wall and rolls towards the wing/wall junction to generate a vortical structure near the nose of the wing. This vortical structure wraps itself around the wing to generate a horse-shoe vortex, which with the pressure gradient generated by the wing results in a highly three-dimensional flow field. In the study a three-simultaneous velocity component LDV probe (Olcmen and Simpson, 1995b) was used to obtain time dependent velocity information at seven stations. The data were next processed to obtain the six Reynolds' stresses, ten triple products and the fifteen quadruple products, as well as the contributions from eight octants to each of these quantities.

The station locations were located outside the horseshoe vortex and at each station data were obtained at thirty logarithmically spaced points by traversing the probe perpendicular to the wall. In this paper the data are used in wall-stress coordinates where the x axis is along the wall-shear-stress direction on the tunnel wall pointing downstream and the y axis is perpendicular to the wall. Figures 2 and 3 show the U and W mean velocities and the shear stresses obtained at selected stations.

Table 1: Definition of the octants and the signs of the fluctuating velocity components in different octants..

Octant/ Signs	u'	v'	w'
1 interaction	+	+	+
2 ejection	-	+	+
3 interaction	-	-	+
4 sweep	+	-	+
5 interaction	+	+	-
6 ejection	-	+	-
7 interaction	-	-	-
8 sweep	+	-	-

The flow field around this particular wing is extremely well documented; detailed references for the flow data used in this study and data for other Reynolds numbers are discussed in papers by Ölçmen and Simpson (1990, 1995, 2001), and Simpson (1996, 2001). All data including surface pressure measurements and surface oil-flow visualizations are presented by Ölçmen et al. (1995a, 1995b).

Definitions of the Octants

A conditional averaging technique was employed to calculate the Reynolds-averaged contributions from fluctuating velocity products to the overall Reynolds averaged velocity product. The octants are defined using the signs of the fluctuating velocity components and are given in Table 1. The octants resulting in positive uv value are named the interaction octants (octants, 1, 3, 5 and 7), while the other octants are named the sweep-ejection octants.

Reynolds-averaged mean velocity components were calculated using the inverse of the local instantaneous velocity magnitude as the weighing factor in order to reduce the bias error in the data. The mean velocity components were then subtracted from the time series data to obtain the fluctuating velocity in time. Fluctuating velocity components with the specified combination of the signs were next used to calculate the contributions from each octant using the same weighing factor used for the mean velocities.

EXTENSION OF NAGANO AND TAGAWA (1988, 1990) MODEL FOR THREE-DIMENSIONAL FLOWS

The Nagano and Tagawa model is based on a non-Gaussian three variable joint probability distribution expressed as an infinite series truncated at a chosen order. Nagano and Tagawa chose to include up to the fourth order velocity products in their analysis. The defined joint probability distribution equation is next used to calculate the individual octant contributions to each second and third order product, as a linear function of various Reynolds-averaged second, third and fourth order products. The model and data comparison requires reduced octant contributions from the measured data and the reduced Reynolds-averaged second, third and fourth order velocity correlations to insert into the model. In the following section the extension of the model to three-dimensional flows is discussed.

Model Description

The statistical model developed by Nagano and Tagawa for a 2DTBL with a passive scalar field uses a non-Gaussian three variable joint probability distribution to calculate velocity products. The joint probability function, $P(\hat{u},\hat{v},\hat{w})$ is also defined using measured second and higher order products. The model uses the correlation coefficients rather than the actual value of the products. All of the velocity products were nondimensionalized with the respective powers of the normal stresses $\overline{u^2}, \overline{v^2}, \overline{w^2}$, (eg. $\overline{u^2 v}$ was divided ($\overline{u^2}\ \sqrt{\overline{v^2}}$), and is shown as, $\overline{\hat{u}^2\hat{v}} = \overline{u^2 v}/(\overline{u^2}\ \sqrt{\overline{v^2}})$). Following their derivation and using the same notation the extension of their model to three-dimensional flows can be described as follows:

The Fourier transform of the joint p.d..f., ψ, can be written as,

$$\psi(\xi,\eta,\zeta) = \int_{-\infty}^{\infty}\int_{-\infty}^{\infty}\int_{-\infty}^{\infty} P(\hat{u},\hat{v},\hat{w}) \exp(i(\hat{u}\xi + \hat{v}\eta + \hat{w}\zeta))d\hat{u}d\hat{v}d\hat{w}$$ a

nd one can obtain the three-dimensional joint p.d.f by inverse transformation of this function.

The function ψ is described in terms of the cumulant k_{pqr} using,

$$i^K k_{pqr} = \frac{\partial^K \ln\psi(\xi,\eta,\zeta)}{\partial\xi^p\ \partial\eta^q\ \partial\zeta^r}\Big|_{\xi=0,\eta=0,\zeta=0}$$

where K=p+q+r, and ξ,η,ζ are the dummy variables. Integration of this equation leads to

$$\psi(\xi,\eta,\zeta) = \exp\Big(\sum_{p,q,r=0}^{\infty} k_{pqr}\,\xi^p\,\eta^q\,\zeta^r\Big)$$

On the other hand the Reynolds averaged flow quantities m_{pqr} can be expressed using the following relation

$$m_{pqr} = \overline{\hat{u}^p\hat{v}^q\hat{w}^r} = \int_{-\infty}^{\infty}\int_{-\infty}^{\infty}\int_{-\infty}^{\infty} \hat{u}^p\hat{v}^q\hat{w}^r P(\hat{u},\hat{v},\hat{w})\,d\hat{u}\ d\hat{v}\ d\hat{w}$$ The

function, ψ, can be expressed in terms of m_{pqr} using,

$$\frac{\partial^K \psi(\xi,\eta,\zeta)}{\partial\xi^p\,\partial\eta^q\,\partial\zeta^r}\Big|_{\xi=\eta=\zeta=0} = i^K m_{pqr}$$

Integration of this equation leads to

$$\psi(\xi,\eta,\zeta) = \sum_{p,q,r=0}^{\infty} \frac{i^K}{p!\,q!\,r!} m_{pqr}\,\xi^p\,\eta^q\,\zeta^r$$

Using the expressions for the ψ obtained in terms of m_{pqr} and the k_{pqr} one can calculate the following relations between m_{pqr} and k_{pqr}.

$m_{001}=0$; $m_{010}=0$, $m_{100}=0$; $m_{002}=1$; $m_{020}=1$; $m_{200}=1$; $m_{000}=1$, $k_{000}=0$ for K=0;

$m_{pqr}=k_{pqr}$ for $1 \le K \le 3$;

$k_{004}=-3+m_{004}$; $k_{013}=-3\ m_{011}+m_{013}$; $k_{022}=-1-2m_{011}^2+m_{022}$; $k_{031}=-3m_{011}+m_{031}$; $k_{040}=-3+m_{040}$; $k_{103}=-3m_{101}+m_{103}$;

$k_{112}=-2m_{011}m_{101}-m_{110}+m_{112}$; $k_{121}=-m_{101}-2m_{011}m_{110}+m_{121}$; $k_{130}=-3m_{110}+m_{130}$; $k_{202}=-2m_{101}^2-m_{200}+m_{202}$;

$k_{211}=-2m_{101}m_{110}-m_{011}m_{200}+m_{211}$; $k_{220}=-2m_{110}^2-m_{200}+m_{220}$;

$k_{301}=-3m_{101}m_{200}+m_{301}$; $k_{310}=-3m_{110}m_{200}+m_{310}$;

$k_{400}=-3+m_{400}$

On the other hand the ψ equation expressed in terms of k_{pqr} can be further written as

$$\psi(\xi,\eta,\zeta) = \exp\Big(-\frac{1}{2}(\xi^2+\eta^2+\zeta^2)\Big) \sum_{p,q,r=0}^{\infty} C_{pqr}\,i^K\,\xi^p\,\eta^q\,\zeta^r$$

Equations relating the k_{pqr} and C_{pqr} can be expressed using the

ψ equation written in terms of k_{pqr} and expanding it into series including the third order terms in the expansion

$\exp(x) = 1 + x + \frac{x^2}{2!} + \frac{x^3}{3!}$, and equating the terms from the ψ equation written in terms of C_{pqr}. The C_{pqr} related to k_{pqr} can be expressed in terms of the m_{pqr} which are the measured Reynolds averaged velocity products including the fourth order terms. The process results in the following relations:

$$C_{000} = 1, C_{001} = 0, C_{002} = 0, C_{003} = \frac{1}{6}\overline{\hat{w}^3},$$

$$C_{004} = \frac{1}{24}(\overline{\hat{w}^4} - 3), C_{010} = 0, C_{011} = \overline{\hat{v}\hat{w}}, C_{012} = \frac{1}{2}\hat{v}\overline{\hat{w}^2}$$

$$C_{013} = \frac{1}{6}(\hat{v}\overline{\hat{w}^3} - 3\overline{\hat{v}\hat{w}}), C_{020} = 0, C_{021} = \frac{1}{2}\overline{\hat{v}^2\hat{w}},$$

$$C_{022} = \frac{1}{4}(\overline{\hat{v}^2\hat{w}^2} - 1), C_{030} = \frac{1}{6}\overline{\hat{v}^3}, C_{031} = \frac{1}{6}(\overline{\hat{v}^3\hat{w}} - 3\overline{\hat{v}\hat{w}}),$$

$$C_{040} = \frac{1}{24}(\overline{\hat{v}^4} - 3), C_{100} = 0, C_{101} = \overline{\hat{u}\hat{w}}, C_{102} = \frac{1}{2}\overline{\hat{u}\hat{w}^2}$$

$$C_{103} = \frac{1}{6}(\overline{\hat{u}\hat{w}^3} - 3\overline{\hat{u}\hat{w}}), C_{110} = \overline{\hat{u}\hat{v}}, C_{111} = \overline{\hat{u}\hat{v}\hat{w}},$$

$$C_{112} = \frac{1}{2}(\overline{\hat{u}\hat{v}\hat{w}^2} - \overline{\hat{u}\hat{v}}), C_{120} = \frac{1}{2}\overline{\hat{u}\hat{v}^2}, C_{121} = \frac{1}{2}(\overline{\hat{u}\hat{v}^2\hat{w}} - \overline{\hat{u}\hat{w}})$$

$$C_{130} = \frac{1}{6}(\overline{\hat{u}\hat{v}^3} - 3\overline{\hat{u}\hat{v}}), C_{200} = 0, C_{201} = \frac{1}{2}\overline{\hat{u}^2\hat{w}},$$

$$C_{202} = \frac{1}{4}(\overline{\hat{u}^2\hat{w}^2} - 1), C_{210} = \frac{1}{2}\overline{\hat{u}^2\hat{v}}, C_{211} = \frac{1}{2}(\overline{\hat{u}^2\hat{v}\hat{w}} - \overline{\hat{v}\hat{w}})$$

$$C_{220} = \frac{1}{4}(\overline{\hat{u}^2\hat{v}^2} - 1), C_{300} = \frac{1}{6}(\overline{\hat{u}^3}), C_{301} = \frac{1}{6}(\overline{\hat{u}^3\hat{w}} - 3\overline{\hat{u}\hat{w}}),$$

$$C_{310} = \frac{1}{6}(\overline{\hat{u}^3\hat{v}} - 3\overline{\hat{u}\hat{v}}), C_{400} = \frac{1}{24}(\overline{\hat{u}^4} - 3)$$

Substituting the C_{pqr} in the ψ equation and by taking the inverse Fourier transform of the resulting equation the probability density function is expressed.

$$P(\hat{u},\hat{v},\hat{w}) = \frac{1}{(2\pi)^3}\int_{-\infty}^{\infty}\int_{-\infty}^{\infty}\int_{-\infty}^{\infty}\psi(\xi,\eta,\zeta)\times$$

$$\times[\exp(-i(\hat{u}\xi + \hat{v}\eta + \hat{w}\zeta))d\xi d\eta d\zeta]$$

$$= \frac{1}{(2\pi)^{3/2}}\sum_{p,q,r=0}^{\infty} C_{pqr} H_p(\hat{u}) H_q(\hat{v}) H_r(\hat{w})\times$$

$$\times[\exp(-\frac{1}{2}(\hat{u}^2 + \hat{v}^2 + \hat{w}^2))]$$

where, $H_k(\chi) = (-1)^k \exp(\frac{1}{2}\chi^2)\frac{d^k}{d\chi^k}\exp(-\frac{1}{2}\chi^2)$

Using this probability function the m_{pqr} can be now calculated. The fractional contributions from each octant to a higher order product can be calculated using

$$(\overline{\hat{u}^l\hat{v}^m\hat{w}^n})_i = \sigma_{u,i}^l \sigma_{v,i}^m \sigma_{w,i}^n \times$$

$$\times[\int_0^{\infty}(\int_0^{\infty}(\int_0^{\infty}\hat{u}^l\hat{v}^m\hat{w}^n P(\sigma_{u,i}\hat{u}\sigma_{v,i}\hat{v}\sigma_{w,i}\hat{w})d\hat{w}d\hat{v}d\hat{u}]$$

where, $\sigma_{u,i}$ =(1,-1,-1,1,1,-1,-1,1); $\sigma_{v,i}$ =(1,1,-1,-1,1,1,-1,-1); $\sigma_{w,i}$ =(1,1,1,1,-1,-1,-1,-1)

The equation for fractional contributions is rewritten as:

$$(\overline{\hat{u}^l\hat{v}^m\hat{w}^n})_i = \frac{1}{(2\pi)^{3/2}}\sum_{p,q,r=0}^{K\le 4}\sigma_{u,i}^{l+p}\sigma_{v,i}^{m+q}\sigma_{w,i}^{n+r} C_{pqr} B_{l,p} B_{m,q} B_{n,r}$$

where, $B_{j,k} = \int_0^{\infty}\chi^j H_k(\chi)\exp(-\frac{1}{2}\chi^2)d\chi$

$B_{0,0} = \sqrt{\frac{\pi}{2}}$, $B_{0,1} = 1$, $B_{0,2} = 0$, $B_{0,3} = -1$, $B_{0,4} = 0$, $B_{1,0} = 1$

$B_{1,1} = \sqrt{\frac{\pi}{2}}$, $B_{1,2} = 1$, $B_{1,3} = 0$, $B_{1,4} = -1$, $B_{2,0} = \sqrt{\frac{\pi}{2}}$, $B_{2,1} = 2$

$B_{2,2} = \sqrt{2\pi}$, $B_{2,3} = 2$, $B_{2,4} = 0$, $B_{3,0} = 2$, $B_{3,1} = 3\sqrt{\frac{\pi}{2}}$

$B_{3,2} = 6$, $B_{3,3} = 6\sqrt{\frac{\pi}{2}}$, $B_{3,4} = 6$

RESULTS AND DISCUSSION

Structural models for third order products

The Nagano Tagawa method which was extended to three-dimensional flows shows that the octant contributions both to the second and third order products are functions of the second, third and fourth order products in general.

The next step in extending Nagano and Tagawa's analysis is examination of the contributions from different octants to see if the derived equations represent the data. Figure 4 shows a good agreement between the experimental and the modeled contributions to each of the ten triple products and the eight octants for station five. While only station five is shown, the other stations show good agreement with the model also.

In this study the first relations between the triple products were obtained by equating the equations for the octants of each of the second order products that closely matched each other as observed from the data: octant 1 was equated to octant 7, octant 3 to octant 5. Additionally, octant 4 was equated to octant 6, and octant 2 to octant 8, although this was observed to be true only in limited regions of the profiles. More relations were obtained by iteratively summing each of the relations with each other to systematically check every available combination of relations and observing their match with the experimental data, although most of the relations were not justified. This process yielded over 3,500 relations and only one relation was found to fairly resemble the data. This relation is given below:

$$-\frac{\pi}{2}\overline{\hat{u}\hat{v}^2} - \pi\overline{\hat{u}\hat{v}\hat{w}} - \frac{\pi}{2}\overline{\hat{u}^2\hat{v}} + \overline{\hat{v}^2\hat{w}} - \frac{1}{3}\overline{\hat{w}^3} + (1-\pi)\overline{\hat{u}^2\hat{w}} = 0$$

Figure 4 also shows that the sum of the contributions to each of the triple products from the interaction octants are nearly negligible. Thus, a second set of relations was obtained by summing the equations for the interaction octants of the triple products and equating to zero. In other words, for each triple product, the first, third, fifth, and seventh octant equations were added to each other. The ten triple products were used to find ten relations in terms of only triple products. These relations were then used to calculate each triple product and were compared with the measured data. It was determined that seven of those relations yielded good agreement with measured data. The seven relations were found from the equations for the triple products $\overline{\hat{u}^2\hat{v}}$, $\overline{\hat{u}^2\hat{w}}$, $\overline{\hat{u}^3}$, $\overline{\hat{u}\hat{v}^2}$, $\overline{\hat{u}\hat{v}\hat{w}}$, $\overline{\hat{v}^2\hat{w}}$, and $\overline{\hat{v}^3}$, and these relations are listed below in the order of the triple stress model equations used to obtain them.

$$\overline{\hat{u}\hat{v}^2} + \frac{\pi}{2}\overline{\hat{u}^2\hat{v}} + \frac{1}{3}\overline{\hat{u}^3} = 0$$

$$\frac{\pi}{4}\overline{\hat{u}^2\hat{w}} + \overline{\hat{u}\hat{v}\hat{w}} = 0$$

$$\overline{\hat{u}^2\hat{v}} - \frac{1}{9}\overline{\hat{v}^3} + \frac{\pi}{6}\overline{\hat{u}^3} = 0$$

$$\overline{\hat{v}^3} + 3\,\overline{\hat{u}^2\hat{v}} + \frac{3\pi}{2}\,\overline{\hat{u}\hat{v}^2} = 0$$

$$\overline{\hat{v}^2\hat{w}} + \overline{\hat{u}^2\hat{w}} + \pi\,\overline{\hat{u}\hat{v}\hat{w}} = 0$$

$$\frac{\pi}{4}\,\overline{\hat{v}^2\hat{w}} + \overline{\hat{u}\hat{v}\hat{w}} = 0$$

$$\pi\,\overline{\hat{v}^3} - \frac{2}{3}\,\overline{\hat{u}^3} + 6\,\overline{\hat{u}\hat{v}^2} = 0$$

Figure 5 shows the comparison between triple product data and results from the seven equations expressed for $\overline{\hat{u}^2\hat{v}}$, $\overline{\hat{u}^2\hat{w}}$, $\overline{\hat{u}^3}$, $\overline{\hat{u}\hat{v}^2}$, $\overline{\hat{u}\hat{v}\hat{w}}$, $\overline{\hat{v}^2\hat{w}}$, $\overline{\hat{v}^3}$ triple products in the order of the equations at stations 2, 5, and 7. Therefore, the first equation was solved for $\overline{\hat{u}^2\hat{v}}$, in terms of $\overline{\hat{u}\hat{v}^2}$ and $\overline{\hat{u}^3}$, the second equation for $\overline{\hat{u}^2\hat{w}}$, and so on. For the $\overline{\hat{u}^2\hat{v}}$, next the experimental data for $\overline{\hat{u}\hat{v}^2}$ and the $\overline{\hat{u}^3}$ were used to obtain a profile and this profile was compared to the experimental $\overline{\hat{u}^2\hat{v}}$ data. These equations could also be used to solve for the other triple product terms. The figure shows that the model and the data agree fairly well. The accuracy of each equation is directly related to the magnitude of the sum of the interaction octants. For many of the triple products, data below y+ of 50 shows significant interaction octant contributions. Thus, the relations show more deviations from data in that region.

Additional relations were derived by using algebraic manipulations of the above relations to express each of the triple products as a function of only one other triple product. As an example, $\overline{\hat{u}^2\hat{v}} = -0.6833\,\overline{\hat{u}^3}$ can be obtained from relations 1, 3 and 4, $\overline{\hat{u}^2\hat{v}} = -0.51488\,\overline{\hat{u}^3}$ can be obtained from relations 1, 4 and 7. Such relations did not give better results than the previously expressed relations.

CONCLUSIONS

The models developed by Nagano and Tagawa are expanded to include three-dimensional flows. Contributions from each of the eight octants obtained for each of the ten triple product correlations show that the contributions from the interaction mode octants (octants, 1, 3, 5, 7) are much smaller in magnitude than the sweep/ejection mode octant contributions. The model developed was successful in expressing the contributions to each octant using the second, third and fourth order fluctuating velocity correlations. The observations such as that the interaction mode contributions are small and that the Nagano-Tagawa model could be used to express the contributions from different octants for a triple product was used to derive relations among the triple products. These derived relations were compared to the available experimental data with success.

REFERENCES

Daly, B.J., and Harlow, F.H., 1970, "Transport equations in turbulence", *Physics of Fluids*, Vol. 13, p. 2634.

Hanjalic, K., and Launder, B.E., 1972, "A Reynolds stress model of turbulence and its applications to asymmetric boundary layers", *J. Fluid Mech.*, Vol. 52, p. 609.

Lemay, J., Bonnet, J.P., and Delville, J., 1995, "Experimental testing of diffusion models in a manipulated turbulent boundary layer", *AIAA Journal*, Vol. 33, No. 9, Sept, pp. 1597-1603.

Lumley, J.L., 1970, *Stochastic Tools in Turbulence*, Academic Press, New York.

Lumley, J.L., 1978, "Computation Modelling of Turbulent Flows", *Adv. in Applied Mech.*, Vol 18., pp. 124-176.

Mellor, G.L., and Herring, H.J., 1973, "A survey of mean turbulent field closure models", *AIAA Journal*, Vol. 11, p. 590.

Nagano Y., and Tagawa M., 1988, "Statistical charateristics of wall turbulence with a passive scalar", *J. Fluid Mech*, Vol 196, pp 157-185.

Nagano Y., and Tagawa M., 1990, "A structural turbulence model for triple products of velocity and scalar", *J. Fluid Mech*, Vol 215, pp 639-657.

Ölçmen, M.S., and Simpson, R.L., 1990, "An Experimental Investigation of a Three-Dimensional Pressure-driven Turbulent Boundary Layer", PhD.Thesis, Virginia Tech, Blacksburg, VA.

Ölçmen, M.S., and Simpson, R.L., 1995, "An experimental study of a three-dimensional pressure-driven turbulent boundary layer", *J. Fluid Mech.*, Vol. 290, pp. 225-262.

Ölçmen, M.S., and Simpson, R.L., 1997, "Experimental evaluation of turbulent diffusion models in complex 3-D flow near a wing/body junction", AIAA 97-0650.

Ölçmen, M.S. , R. L. Simpson , and J. George, 2001, "Some Reynolds number effects on two- and three-dimensional turbulent boundary layers", *Experiments in Fluids* , Vol. 31, Issue 2, pp. 219-228.

Schwarz, W.R., and Bradshaw, P., 1994, "Term-by-term tests of stress-transport turbulence models in a three-dimensional boundary layer", *Physics of Fluids,* Vol. 6, No. 2, pp. 986-999.

Simpson, R.L., 1996, "Aspects of Turbulent Boundary Layer Separation", *Progress in Aerospace Sciences*," Vol. 32, pp.457 – 521.

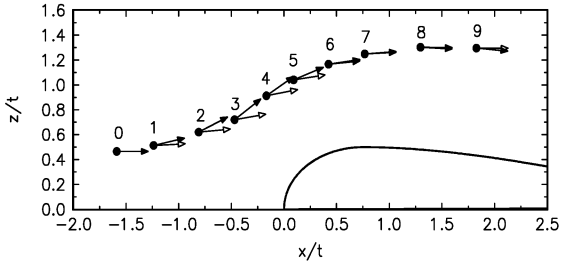

Figure 1: Schematic figure of the wing-body junction. The dots show the measurement locations. Full arrows in wall-stress direction. Empty arrows in free-stream direction.

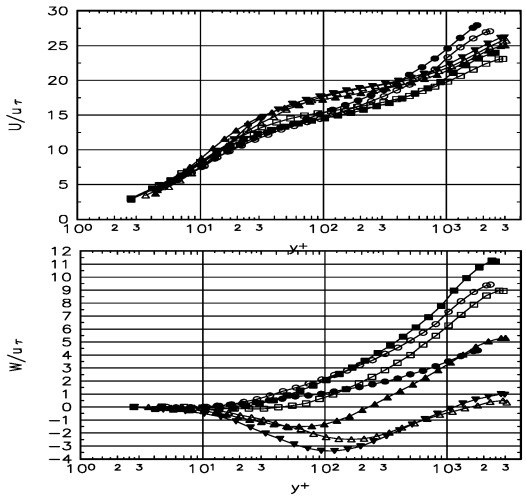

Figure 2. U and W components of the velocity presented in wall-stress coordinates. •,station1; o,station2; ■, station3; □, station4; ▲, station5; ▼, station6; △, station 7

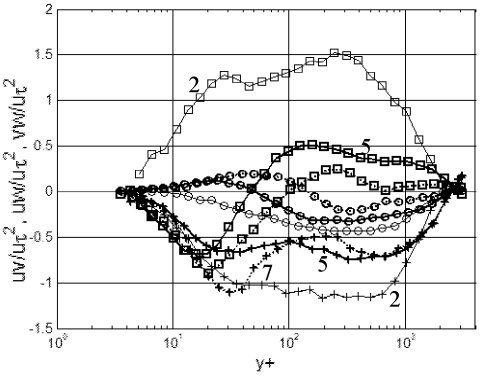

Figure 3. Shear stresses presented in wall-stress coordinates at selected stations. □, $\overline{uw}$; o, $\overline{vw}$; +, $\overline{uv}$; solid line station 2; thick solid line, station 5; dashed line station 7.

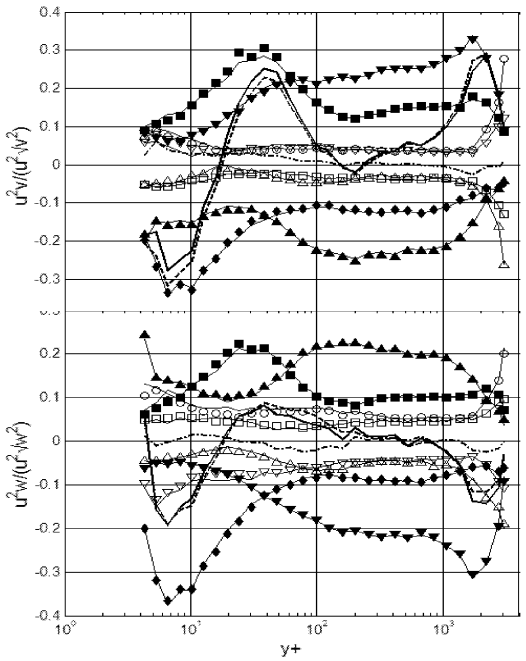

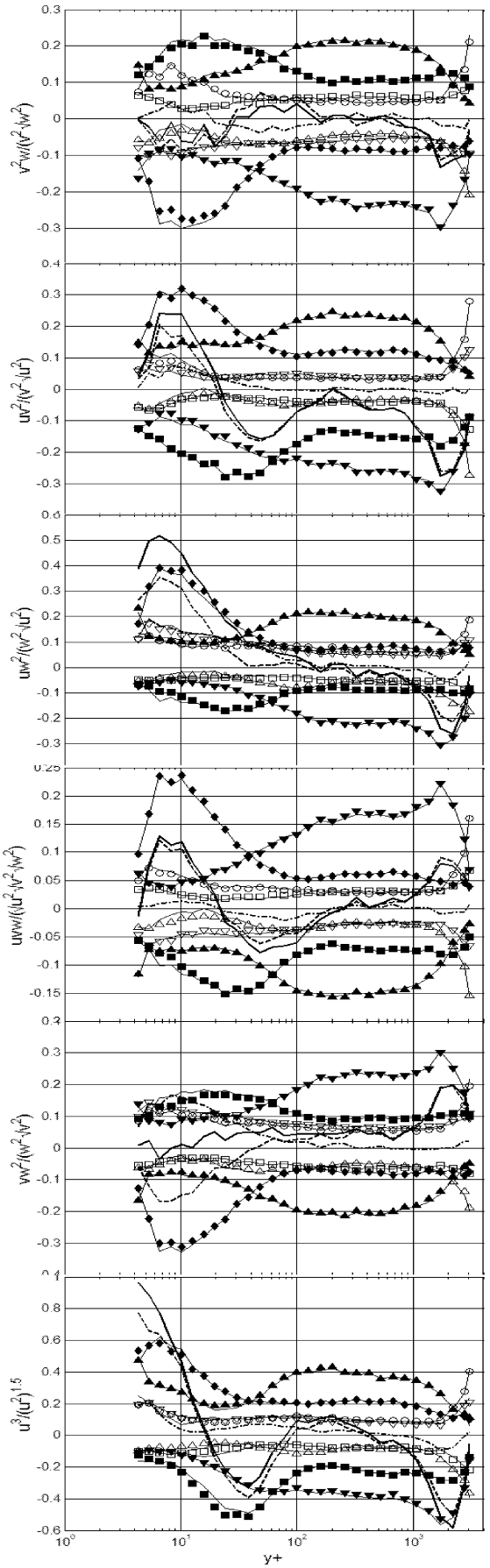

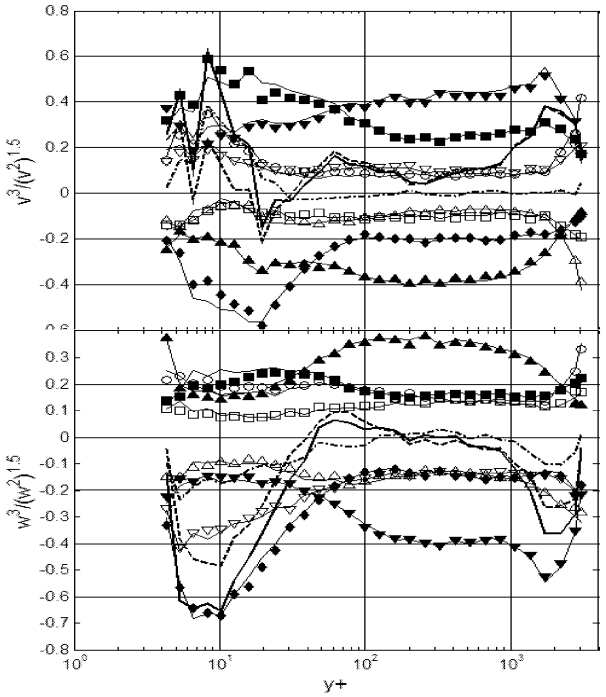

Figure 4. Non-dimensional triple products, Nagano-Tagawa model predictions for each octant, contributions from each octant, contributions from interaction and sweep/ejection octants for ten triple products presented for Station 5. Symbols show experimental data, octants 1 through 8, ○, ■, □, ▲,▽, ▼, △, ◆. Solid lines following the symbols show octant contribution predictions using model. Thick-solid line shows the non-dimensional triple product. Dashed line shows contributions from sweep/ejection octants modes. Dot-dash line shows contributions from interaction modes.

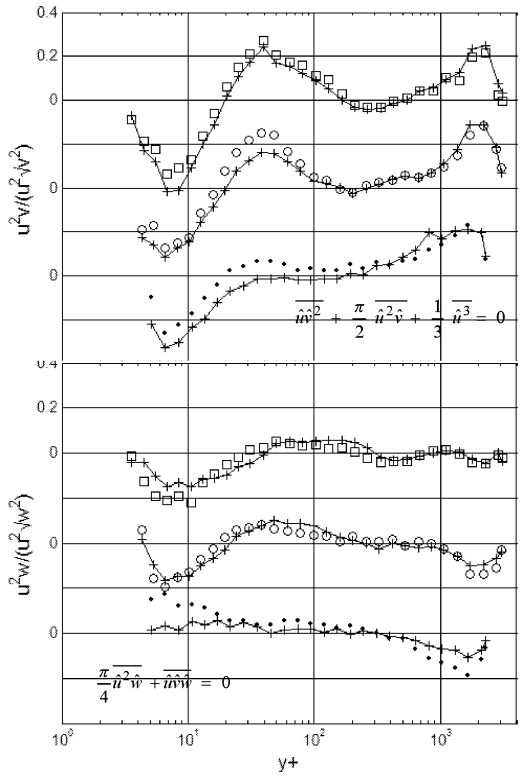

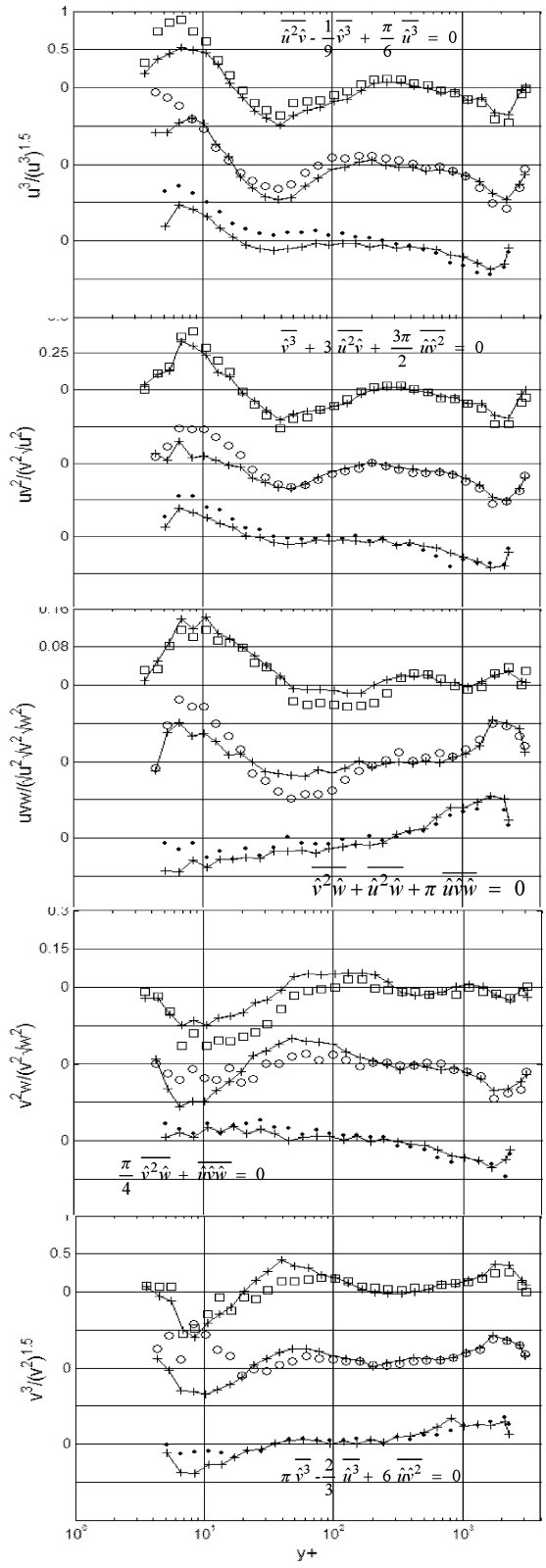

Figure 5. Comparison between the seven models and the experimental data for Stations 2, 5 and 7. Experimental data for station 2, 5, and 7 are shown by, •, ○, and, □ respectively. Lines together with, + symbol show the model predictions. Equations used to obtain the plotted triple product is shown in the figure.